

transitions, to give finally a  $\Delta M_S = -1/2 \rightarrow 1/2$  transition at 100 K. EPR spectra of frozen green-brown solutions obtained by dissolving the green complex in solvents such as DMF,  $\text{Me}_2\text{SO}$ , or  $\text{CH}_3\text{CN}$  gives a typical mixed-valence 16-line pattern. Magnetochemistry studies show that  $\mu_{\text{eff}}/\text{Mn}$  for the green powder decreases from 2.1  $\mu_B$  at 300 K to 0.71  $\mu_B$  at 1.9 K. An intramolecular antiferromagnetic interaction with  $J = -54 \text{ cm}^{-1}$  was found on fitting the experimental data to the equations for an exchange interacting ( $S_1 = 5/2, S_2 = 2$ ) dimer.

Variable-temperature susceptibility results (from 5.9  $\mu_B$  at 300 K to 1.86  $\mu_B$  at 1.7 K) for a solid sample of the  $\text{Mn}^{\text{II}}$ (saldien) complex indicate a dimeric structure, i.e.,  $[\text{Mn}^{\text{II}}(\text{saldien})]_2$ , which is probably similar to that reported<sup>8</sup> for  $[\text{Cu}^{\text{II}}(\text{saldien})]_2$ . Compared to the IR spectrum of  $\text{Mn}^{\text{II}}[5\text{-NO}_2(\text{saldien})]$ , the CsBr pellet IR spectrum of the green  $\text{O}_2$  oxidation product exhibits two peaks at 657 and 793  $\text{cm}^{-1}$  which may be respectively assigned to the Mn-O and the O-O stretching vibrations of a coordinated peroxide group. When the green  $\text{O}_2$  oxidation product is heated (180 °C) under vacuum, the color of the powder turns back from green to orange which is the color of  $\text{Mn}^{\text{II}}[5\text{-NO}_2(\text{saldien})]$ . Furthermore, the EPR characteristics (solid state and frozen solution) of the orange solid and  $\text{Mn}^{\text{II}}[5\text{-NO}_2(\text{saldien})]$  are identical. Efforts are continuing to grow good crystals of the green compound. Taking into account the fact that the  $\text{O}_2$  oxidation of  $\text{Mn}^{\text{II}}$  complexes with ligands such as saldien gives  $\text{Mn}^{\text{III}}$  as the most oxidized form of the manganese,<sup>9</sup> we suggest that the green compound consists of two  $\text{Mn}^{\text{II}}\text{Mn}^{\text{III}}(\text{saldien})_2$  units bridged by an  $\text{O}_2^{2-}$  ion.<sup>10</sup>

The frozen-solution EPR spectra of our mixed-valence complexes were simulated in the same manner<sup>11</sup> as employed by Cooper et al.<sup>7</sup> The lower trace (B) in Figure 1 shows the best simulated spectrum obtained for a pair of inequivalent manganese ions; i.e., the  $\text{Mn}^{\text{II}}\text{Mn}^{\text{III}}$  complex has a localized structure. Small anisotropies in the manganese  $A$  and  $g$  tensors were incorporated to get the best simulation. The final parameters for the ground-state Kramers doublet of the pair are  $g_x = g_y = 2.006$  and  $g_z = 2.00$ ;  $A_{1x} = A_{1y} = 170 \text{ G}$  and  $A_{1z} = 156 \text{ G}$ ;  $A_{2x} = A_{2y} = A_{2z} = 83 \text{ G}$ . We can recast these hyperfine values into the single-ion values. If the complex is incorrectly assumed to be a  $\text{Mn}^{\text{III}}\text{Mn}^{\text{IV}}$  complex, we find  $A_x = A_y = 85 \text{ G}$  and  $A_z = 78 \text{ G}$  for  $\text{Mn}^{\text{III}}$  whereas  $A_x = A_y = A_z = 83 \text{ G}$  for  $\text{Mn}^{\text{IV}}$ . If the complex is correctly assumed to be a  $\text{Mn}^{\text{II}}\text{Mn}^{\text{III}}$  complex  $A_x = A_y = 73 \text{ G}$  and  $A_z = 67 \text{ G}$  for  $\text{Mn}^{\text{II}}$  whereas  $A_x = A_y = A_z = 62 \text{ G}$  for  $\text{Mn}^{\text{III}}$ . The hyperfine interaction calculated for the  $\text{Mn}^{\text{IV}}$  ion (83 G) in the  $\text{Mn}^{\text{III}}\text{Mn}^{\text{IV}}$  formulation does not agree with the 97 G hyperfine interaction we have determined<sup>12</sup> for a frozen solution of  $(\text{Mn}^{\text{IV}}[5\text{-NO}_2(\text{saldien})](\text{ClO}_4)_2$ , a mononuclear compound that was prepared electrochemically. For a frozen solution of  $\text{Mn}^{\text{II}}[5\text{-NO}_2(\text{saldien})]$ , we find a dimer-type EPR signal with an 11-line  $S = 0$  to  $S = 1$  manganese hyperfine pattern with a splitting of  $A = 38 \text{ G}$ . A value that is twice this dimer interaction (i.e., 76 G) is in better agreement with the 73 G interaction found for the  $\text{Mn}^{\text{II}}$  ion in the  $\text{Mn}^{\text{II}}\text{Mn}^{\text{III}}$  formulation.

The above analysis suggests that caution has to be exercised in deciding which oxidation states of manganese are present in

a mixed-valence complex if only the magnitudes of manganese hyperfine interactions are known from EPR simulations. It is quite possible that the hyperfine interaction can vary considerably for a given oxidation state of manganese depending on the coordination number and geometry of the manganese ion.

**Acknowledgment.** We thank the National Institutes of Health for partial support of the work at the University of Illinois through a Grant HL13652 to D.N.H. Tuchagues and Hendrickson are thankful for a NATO grant for collaborative research. Helpful discussions with Dr. M. J. Nilges about EPR simulations are acknowledged.

### Characterization of Transient Intermediates on Laser Flash Excitation of Cyclohexenones in the Presence of Amines<sup>1</sup>

D. A. Dunn and D. I. Schuster\*

Department of Chemistry, New York University  
New York, New York 10003

R. Bonneau\*

Laboratoire de Chimie Physique  
Université de Bordeaux 1, 33405 Talence, France

Received October 15, 1984

Recently, we reported that upon laser flash photolysis of a series of 2-cyclohexenones, transient absorption could be observed in the ultraviolet region (260–320 nm) whose lifetime correlates with the ability of the enone to twist about the  $\text{C}_2\text{-C}_3$  double bond.<sup>2</sup> This structural feature also determines the rate of energy transfer to triplet quenchers such as naphthalene (NA), 1,3-cyclohexadiene (CHD), and piperylene.<sup>3</sup> Olefins such as 1,1-dimethoxyethylene (DME) and cyclohexene and amines such as 1,4-diazabicyclo-[2.2.2]octane (DABCO) and triethylamine quench certain photoreactions of these enones but have no effect on the observed transient.<sup>2</sup> We therefore concluded that for conformationally flexible enones, this transient does not lead to photoproducts.<sup>4</sup> A "phantom" triplet state, which has not yet been directly detected, was proposed to be responsible for reaction with amines and olefins, as well as triplet energy transfer to NA and CHD.<sup>2</sup> For conformationally rigid enones, the distinction between the spectroscopically observable species and the chemically reactive triplet state becomes blurred.

We now report that flash photolysis of degassed samples of enones 1–5 in acetonitrile in the presence of tertiary amines using a 353-nm pulse from a mode-locked Nd:YAG laser yielded new long-lived transients absorbing from 260 to 500 nm. Figure 1 shows spectra generated from enones 1, 2, and 4 in the presence of DABCO and *N,N*-dimethylaniline (DMA).

Flash excitation of DABCO alone in acetonitrile with a 265-nm pulse produces a broad absorption which decays with a lifetime of 22 ns and narrow absorption which decays with  $\tau = 4\text{--}7 \mu\text{s}$ ,

(8) McKenzie, E. D.; Selvey, S. J. *Inorg. Chim. Acta* 1976, 18, L1–L2.

(9) (a) Coleman, W. M.; Taylor, L. T. *Inorg. Chem.* 1977, 16, 1114–1119.

(b) Coleman, W. M.; Taylor, L. T. *Inorg. Chim. Acta* 1978, 30, L291–L293.

(10) Peroxide-bridged binuclear manganese complexes have been suggested by Coleman and Taylor for the oxygenation products of the related  $\text{Mn}^{\text{II}}$ (XSaldDPT) compounds.<sup>9b</sup>

(11) (a) The frozen-glass, X-band, EPR spectra were simulated employing the following spin Hamiltonian:  $\hat{H} = g\beta H_z \hat{S}_z + g\beta(H_x \hat{S}_x + H_y \hat{S}_y) + \lambda \hat{A} \hat{S}$ . The EPR signal is attributable to the ground-state Kramers doublet resulting from an antiferromagnetic exchange interaction between two Mn ions. In the simulation a Gaussian line shape was assumed with the line width of a particular transition determined by the nuclear spin quantum number and the degree of strain in  $g$  and  $A$  tensors. A computer program based on the following sources was employed: (a) Nilges, M. J. Ph.D. Thesis, University of Illinois, Urbana, IL 1979. (b) Belford, R. L.; Nilges, M. J. "Computer Simulation of Powder Spectra", EPR symposium, 21st Rocky Mountain Conference, Denver, CO, 1979. (c) Maurice, A. M. Ph.D. Thesis, University of Illinois, Urbana, IL, 1980.

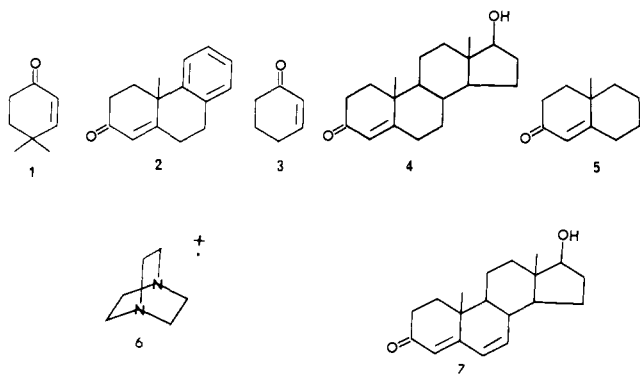
(12) Mabad, B.; de Montauzon, D.; Tuchagues, J.-P.; Hendrickson, D. N., manuscript in preparation which includes single-crystal X-ray structural results for a monomeric  $\text{Mn}^{\text{IV}}$  complex.

(1) Part 74 of the NYU series on the photochemistry of ketones in solutions Part 73: Brisimitzakis, A. C.; Schuster, D. I.; van der Veen, J. M. *Can J. Chem.*, in press. Part 72: Schuster, D. I.; Bonneau, R.; Dunn, D. A.; Rao, J. M.; Jousset-Dubien, J. *J. Am. Chem. Soc.* 1984, 106, 2706. Part 71: Schuster, D. I.; Greenberg, M. M.; Nuñez, I. M.; Tucker, P. C. *J. Org. Chem.* 1983, 48, 2615.

(2) (a) Schuster, D. I.; Bonneau, R.; Dunn, D. A.; Rao, J. M.; Jousset-Dubien, J. *J. Am. Chem. Soc.* 1984, 106, 2706. (b) For a review and background references, see: Schuster, D. I. In "Rearrangements in Ground and Excited States"; de Mayo, P., Ed.; Academic Press: New York, 1980; Vol. 3, Essay 17.

(3) For rigid enones such as 4, quenching of the transient absorption at 280 nm by piperylene can be observed directly. However, for flexible enones (e.g., 1 and 3) quenching of this transient by piperylene is inefficient and nonlinear, while no quenching by CHD is observed. Quenching by NA cannot be directly measured at 280 nm due to NA ground-state absorption, but absorption of <sup>3</sup>NA\* at 413 nm is easily monitored.<sup>2a</sup>

(4) Similar conclusions have been reached by Pienta based on complementary studies. See: Pienta, N. J. *J. Am. Chem. Soc.* 1984, 106, 2704.



both centered at  $\sim 460$  nm. In the presence of electron acceptors such as  $N_2O$  or methylviologen, the broad absorption disappeared; in the latter case, the absorption spectrum of the methylviologen radical cation ( $\lambda_{\max}$  603 nm)<sup>5</sup> was observed. We therefore conclude that the broad absorption is due to solvated electrons and that the long-lived absorption is due to solvated DABCO radical cations (6). The latter are reported to absorb strongly around 465 nm with  $\epsilon_{\max}$  2100 M<sup>-1</sup> cm<sup>-1</sup><sup>6a</sup> and have an absorption spectrum in rigid glasses at 77 K<sup>6b,c</sup> very similar to that which we observe in acetonitrile in the presence of  $N_2O$ .

The transient spectra in Figure 1 generated on excitation of the enones in the presence of DABCO are remarkably similar to that assigned to DABCO<sup>+</sup> (6). We therefore conclude that under these conditions electron transfer occurs to give solvated enone radical anions and 6. This is supported by the observation that the lifetimes of the long-wavelength transients are all essentially equal (Table I). This is a rare case of direct observation of amine radical cations generated from ketone excited states in solution. Roth<sup>7</sup> has obtained CIDNP evidence for the intermediacy of radical ions in photoreactions of benzophenone derivatives and amines, while Peters<sup>8</sup> observed the UV absorption of radical anions of aromatic ketones formed in the presence of amines using picosecond laser spectroscopy.<sup>9</sup> Scaiano<sup>10</sup> has observed absorption at 480–590 nm on laser flash excitation of acetophenone in the presence of cyclic 1,5-diamines, attributed to the corresponding diamine radical cations.

For enones 1, 3, and 4 at concentrations sufficient to give an optical density of 0.7–1.0 at 353 nm, plots of the rate of formation of 6 (i.e.,  $1/\tau_{\text{growth}}$ ) were linear with [DABCO], providing rates of quenching ( $k_a$ ) and extrapolated lifetimes ( $\tau_0$ ) of the enone triplet precursors (Table I). These lifetimes are comparable with those obtained from analogous experiments<sup>2</sup> involving rates of transfer of triplet excitation from enones to NA in isopropyl alcohol (Table I). The rise time of the enone 2–DABCO transient was reduced in the presence of DME, corresponding to a quenching rate constant of  $1.2 \times 10^8$  M<sup>-1</sup> s<sup>-1</sup> ( $\pm 50\%$ ), in rough agreement with the previously determined rate constant for interception of the reactive "phantom" triplet of 1 by DME.<sup>2,11</sup> We therefore conclude that electron transfer occurs from DABCO to the same enone triplet state that is quenched by NA and olefins and that undergoes the lumiketone photorearrangement.<sup>2,11,12</sup>

With other tertiary amines, specifically triethylamine and *N,N*-dimethylaniline (DMA), long-lived transients are also seen

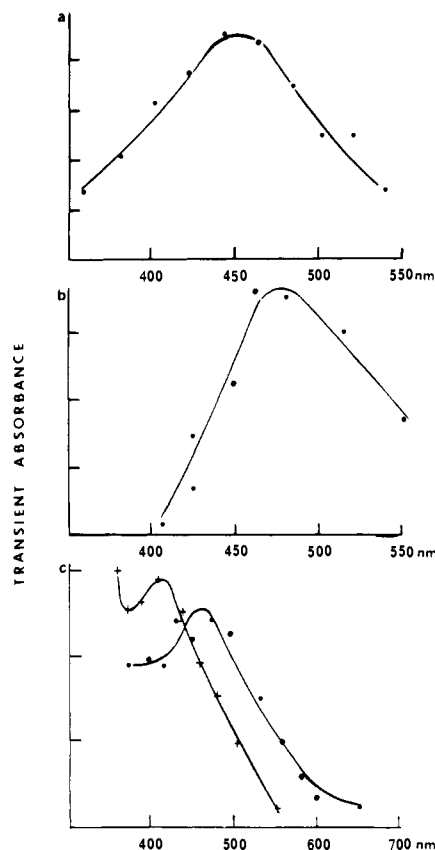


**Figure 1.** Absorption spectra of transient species generated upon laser flash excitation at 353 nm of enones 1 (a), 2 (b), and 4 (c) in the presence of 0.02 M DABCO (●) and 0.01 M DMA (+). Optical densities of the transients produced from 1 and 2 in the presence of DABCO were measured 180 ns after the flash, while, in the case of 4, measurements were made 150 and 600 ns after the laser pulse using DABCO and DMA, respectively.

**Table I.** Kinetic Properties of Transient Enone–DABCO Species<sup>a</sup>

| enone | $\tau_{450}$ , $\mu\text{s}$ | $\tau_0$ , <sup>b</sup> ns | $k_a$ , <sup>b</sup> M <sup>-1</sup> s <sup>-1</sup> | $\tau_0$ , ns <sup>c</sup> |
|-------|------------------------------|----------------------------|--|----------------------------|
| 4     | 1.4–1.9                      | 323                        | $1.2 \times 10^9$                                    | 145 <sup>d</sup>           |
| 1     | 1.0–1.5                      | 19                         | $2.7 \times 10^8$                                    | 28 <sup>d</sup>            |
| 3     | 1.0–1.5                      | 16.9                       | $3.7 \times 10^8$                                    | 24 <sup>e</sup>            |

<sup>a</sup>Numbers are averages of several independent determinations. Estimated experimental uncertainty is 10%. <sup>b</sup>Determined from intercept of plot of  $1/\tau_{\text{growth}}$  vs. [amine] in acetonitrile. <sup>c</sup>Determined from intercept of plot of rise time of triplet naphthalene absorption at 413 nm vs. [NA]. <sup>d</sup>Solvent was isopropyl alcohol. <sup>e</sup>Solvent was acetonitrile.

at long wavelengths. We believe that these are not amine radical cations, which ought to be very short-lived because of rapid proton transfer to the enone radical anions, a process that is inhibited structurally in the case of DABCO.<sup>13</sup> It is likely that the DMA-based transient absorption in Figure 1c is the radical  $\text{PhN}(\text{CH}_3)\text{CH}_2$ , and not  $\text{DMA}^+$ , which has a reported absorption maximum at 460 nm.<sup>6b,14</sup> Our spectrum for this radical agrees with that reported by Scaiano.<sup>15</sup>

The dependence of  $k_a$  for DABCO on enone structure is shown in Table I. The rate of electron donation from DABCO will depend on the excitation energy of the enone triplet acceptor.<sup>16</sup>

(5) Kosower, E. M.; Cotter, J. L. *J. Am. Chem. Soc.* **1964**, *86*, 5524.

(6) (a) Davis, G. T.; Demek, M. M.; Rosenblatt, D. H. *J. Am. Chem. Soc.* **1972**, *94*, 3321. (b) Shida, T.; Nosaka, Y.; Kato, T. *J. Phys. Chem.* **1978**, *82*, 695. Lanyiova, Z. Doctoral Thesis, University of Basel, Switzerland, 1977.

(7) Roth, H. D.; Lamola, A. A. *J. Am. Chem. Soc.* **1974**, *96*, 6270.

(8) Peters, K. S.; Freilich, S. C.; Schaeffer, C. G. *J. Am. Chem. Soc.* **1980**, *102*, 5701. Simon, J. D.; Peters, K. S. *Ibid.* **1981**, *103*, 6403.

(9) See also: Wagner, P. J.; Thomas, M. J. *J. Am. Chem. Soc.* **1980**, *102*, 4173. Masuhara, H.; Maeda, Y.; Mataga, N.; Tomita, K.; Tatsumi, H.; Sakata, Y.; Misumi, S. *Chem. Phys. Lett.* **1980**, *69*, 182. Yates, S. F.; Schuster, G. B. *J. Org. Chem.* **1984**, *49*, 3349.

(10) Scaiano, J. C.; Stewart, L. C.; Livant, P.; Majors, A. W. *Can. J. Chem.* **1984**, *62*, 1339.

(11) Schuster, D. I.; Greenberg, M. M.; Nunez, I. M.; Tucker, P. C. *J. Org. Chem.* **1983**, *48*, 2615.

(12) Nunez, I. M. Ph.D. Dissertation, New York University, 1982.

(13) Inbar, S.; Linschitz, H.; Cohen, S. G. *J. Am. Chem. Soc.* **1981**, *103*, 1048.

(14) Habersbergerova, A., et al., *Radiat. Res. Rev.* **1968**, 109.

(15) Scaiano, J. C. *J. Phys. Chem.* **1981**, *85*, 2851.

(16) Weller, A. *Pure Appl. Chem.* **1968**, *16*, 115. Rehm, D.; Weller, A. *Isr. J. Chem.* **1970**, *8*, 259. It is assumed that variations in electron affinity of the enones with changes in structure are relatively small. The reduction potential of enone 1 in acetonitrile is  $-2.6$  V, as measured by Prof. M. A. Fox, University of Texas.

The observation that  $k_a$  for enone **4** is greater than that for the monocyclic enones (Table I) is consistent with the earlier proposal<sup>17</sup> that the energy of the reactive  $\pi, \pi^*$  triplet of these enones decreases as the ability of the triplet to relax by twisting about the C<sub>2</sub>-C<sub>3</sub> bond increases. Furthermore, the low-energy ( $E_T$  ca. 50 kcal/mol) long-lived (ca. 10  $\mu$ s) triplet state of steroidal dienone **7** is not quenched by DABCO, since electron transfer in this case would be highly endothermic.<sup>18</sup>

We conclude from this study that amines react with relaxed enone  $\pi, \pi^*$  triplet states by the transfer of an electron and formation of solvated enone radical anions and amine radical cations. In the case of DABCO, the exclusive fate of the radical ion pair appears to be decay to the ground state since no enone-DABCO adducts have as yet been detected, although enone-amine adducts and reduced enone are formed when other tertiary amines are utilized.<sup>19,20</sup>

**Acknowledgment.** This collaboration was made possible by Grant 0418/83 from the NATO Scientific Affairs Division. We also gratefully acknowledge support of this work by the donors of the Petroleum Research Fund, administered by the American Chemical Society, and by the National Science Foundation (CHE-8320154).

**Registry No.** **1**, 1073-13-8; **2**, 6606-34-4; **3**, 930-68-7; **4**, 58-22-0; **5**, 826-56-2; DABCO, 280-57-9; DMA, 121-69-7.

(17) Bonneau, R. *J. Am. Chem. Soc.* **1980**, *102*, 3816.

(18) Schuster, D. I.; Dunn, D. A.; Bonneau, R. *J. Photochem.*, in press.

(21) Dunn, D. A.; Schuster, D. I., unpublished results.

(22) See also: Pienta, N. J.; McKimney, J. E. *J. Am. Chem. Soc.* **1982**, *104*, 5501.

## Spectroscopic Determination of $\sigma_I$ and $\sigma_R$ Substituent Constants for the Deuterium Atom

H. Künzer and S. Berger\*

Fachbereich Chemie der Universität Marburg  
D-3550 Marburg, West Germany

Received October 16, 1984

Deuterium-induced differences  $\Delta\delta$  in the chemical shifts of carbon atoms of isotopomeric molecules have been investigated by <sup>13</sup>C NMR spectroscopy for a number of reasons.<sup>1,2</sup> As a consequence of the Born-Oppenheimer approximation their origin should always be attributed to the difference in vibrational motion of the two isotopes. Yet, the interpretation of the observed isotope-induced shifts is often given in terms of electronic substituent effects. Thus, for example, shifts to lower field of carbon atoms in ortho and para position in side-chain deuterated alkyl derivatives of benzenes<sup>3</sup> as well as the dependence of the shifts of both ortho positions of several trideuteriomethylated aromatic systems on  $\pi$ -bond order<sup>4</sup> have been taken as a manifestation of isotopic perturbation of hyperconjugation. In extension of our earlier work<sup>5</sup> we have recently discussed isotope-induced  $\pi$ -polarization to account for the experimental results in a series of deuterated derivatives of biphenyl.<sup>6</sup>

The behavior of the carbon atoms in the unsaturated side chain of the styrene derivatives **1a**, **2a**, and **3a** (X = D), which constitutes

(1) Batiz-Hernandez, H.; Bernheim, R. A. *Prog. Nucl. Magn. Reson. Spectrosc.* **1967**, *3*, 63-85.

(2) Hansen, P. E. *Annu. Rep. NMR Spectrosc.* **1983**, *15*, 105-234.

(3) Wesener, J. R.; Günther, H. *Tetrahedron Lett.* **1982**, 2845-2848. Schaefer, T.; Peeling, J.; Wildman, T. A. *Can. J. Chem.* **1983**, *61*, 2777-2778.

(4) Ernst, L.; Hopf, H.; Wullbrandt, D. *J. Am. Chem. Soc.* **1983**, *105*, 4469-4470.

(5) Berger, S.; Künzer, H. *Tetrahedron* **1983**, *39*, 1327-1329. Berger, S.; Künzer, H. *Angew. Chem.* **1983**, *95*, 321-322; *Angew. Chem., Int. Ed. Engl.* **1983**, *22*, 321-322.

(6) Künzer, H.; Berger, S. *Tetrahedron Lett.* **1984**, *25*, 5019-5022.

Table I. Long-Range Deuterium Isotope Effects  $\Delta\delta$  on <sup>13</sup>C Chemical Shifts<sup>a</sup> and Substituent Susceptibilities  $\rho_{I,R}$  from DSP Analysis<sup>b</sup>

| compd | C-5  | C-6                  | C-7               | C-8               | C-9               | ref |
|-------|--|----------------------|-------------------|-------------------|-------------------|-----|
|       | $\Delta\delta$ -8<br>$\rho_I^i$ -2.39<br>$\rho_R^i$ -0.36  | 12<br>4.97<br>8.89   |                   |                   |                   | 10  |
|       | $\Delta\delta$ -8<br>$\rho_I^i$ -1.83<br>$\rho_R^i$ 0.15   | 9<br>4.03<br>6.97    |                   |                   |                   | 10  |
|       | $\Delta\delta$ -9<br>$\rho_I^i$ -1.99<br>$\rho_R^i$ -0.36  | 0<br>1.91<br>0.99    |                   |                   |                   | 10  |
|       | $\Delta\delta$ -6<br>$\rho_I^i$ -5.3<br>$\rho_R^i$ 1.23    | 0<br>-0.73<br>0.21   | 0<br>0.26<br>0.17 | 0<br>1.15<br>0.12 |                   | 16  |
|       | $\Delta\delta$ -10<br>$\rho_I^i$ -3.17<br>$\rho_R^i$ -1.14 | 0<br>0.41<br>1.11    | 0<br>0.49<br>0.26 | 4<br>2.00<br>2.09 |                   | 17  |
|       | $\Delta\delta$ -5<br>$\rho_I^i$ -2.31<br>$\rho_R^i$ 0.52   | -4<br>-1.63<br>-1.83 |                   |                   | 0<br>1.35<br>1.28 | 18  |
|       | $\Delta\delta$ -8<br>$\rho_I^i$ -2.9<br>$\rho_R^i$ -1.8    | 15<br>5.1<br>6.1     |                   |                   |                   | 19  |

<sup>a</sup> Data given in ppb, spectra recorded at 100.6 MHz on a Bruker WH-400 spectrometer in acetone-*d*<sub>6</sub> solutions. All solutions contained unequal amounts of deuterated and parent compounds, errors amount to 0.75 ppb. The sign of the isotope effects follows the convention given by Hansen<sup>2</sup> and is, unfortunately, opposite to the convention used for substituent effects ( $\text{SCS}^i = \delta_{\text{RX}}^i - \delta_{\text{RH}}^i$  and  $\Delta\delta = \delta_{\text{RH}}^i - \delta_{\text{RD}}^i$ ).

a definitive experimental test of our proposal, is reported here along with an attempt to correlate a number of long-range deuterium isotope effects with data from studies of common substituent effects.

The para-substituent-induced chemical shift (SCS) of the carbon atoms of the vinyl sidechain in **1-3** has been analyzed by the DSP method<sup>7-9</sup> by Reynolds and co-workers.<sup>10</sup> The effect of substituents X on the chemical shifts of the vinyl carbon atoms is given by eq 1. The parameters  $\rho_I^i$  and  $\rho_R^i$  measure the sus-

$$\text{SCS}^i = \rho_I^i \sigma_{I,X} + \rho_R^i \sigma_{R,X} \quad (1)$$

ceptibility of the *i*th carbon atom on the polar ( $\sigma_{I,X}$ ) and mesomeric ( $\sigma_{R,X}$ ) nature of the substituent X.  $\rho_I^i$  and  $\rho_R^i$  values obtained from statistical analysis are included in Table I for compounds **1-7**. All C-6 atoms of **1-3** show a pronounced susceptibility to the mesomeric influence of substituents X. As the conjugation between the phenyl ring and the vinyl group is diminished by steric

(7) Ehrenson, S.; Brownlee, R. T. C.; Taft, R. W. *Prog. Phys. Org. Chem.* **1973**, *10*, 1-80.

(8) Reynolds, W. F. *Prog. Phys. Org. Chem.* **1983**, *14*, 165-203.

(9) Craik, D. J.; Brownlee, R. T. C. *Prog. Phys. Org. Chem.* **1983**, *14*, 1-73.

(10) Hamer, G. K.; Peat, J. R.; Reynolds, W. F. *Can. J. Chem.* **1973**, *51*, 897-914, 915-926.